AIP Applied Physics Letters

Effects of nanoparticle deposition on surface wettability influencing boiling heat transfer in nanofluids

S. J. Kim, I. C. Bang, J. Buongiorno, and L. W. Hu

Citation: Applied Physics Letters **89**, 153107 (2006); doi: 10.1063/1.2360892

View online: http://dx.doi.org/10.1063/1.2360892

View Table of Contents: http://scitation.aip.org/content/aip/journal/apl/89/15?ver=pdfcov

Published by the AIP Publishing

Effects of nanoparticle deposition on surface wettability influencing boiling heat transfer in nanofluids

S. J. Kim, I. C. Bang, J. Buongiorno,[a] and L. W. Hu
Massachusetts Institute of Technology, Cambridge, Massachusetts 02139

(Received 13 June 2006; accepted 22 August 2006; published online 10 October 2006)

Buildup of a porous layer of nanoparticles on the heated surface occurs upon boiling of nanofluids containing alumina, zirconia, or silica nanoparticles. This layer significantly improves the surface wettability, as shown by a reduction of the static contact angle on the nanofluid-boiled surfaces compared with the pure-water-boiled surfaces. The contact angle reduction is attributed to changes in surface energy and surface morphology brought about by the presence of the nanoparticle layer. The high surface wettability can plausibly explain the boiling critical heat flux enhancement in nanofluids. © *2006 American Institute of Physics*. [DOI: 10.1063/1.2360892]

Nanofluids are engineered colloidal suspensions of nanoparticles in a base fluid[1] and exhibit a very significant enhancement (up to 200%) of the boiling critical heat flux (CHF) at modest nanoparticle concentrations.[2–7] Since CHF is the upper limit of nucleate boiling, such enhancement offers the potential for major performance improvement in many practical applications that use nucleate boiling as their prevalent heat transfer mode. For example, the use of nanofluids with higher CHF could enable effective thermal management of ever smaller and more powerful electronic devices, enable power uprates in commercial nuclear plants, allow design of more compact heat exchangers for the chemical industry, etc. To study the two-phase heat transfer characteristics of nanofluids, we have conducted pool boiling experiments with water-based nanofluids containing Al_2O_3, ZrO_2, and SiO_2 nanoparticles at volume concentrations of 0.1%, 0.01%, and 0.001% (total of nine nanofluids). The nanofluids were prepared by dilution of concentrated (10 wt %) nanofluids purchased from various vendors. The size (effective diameter) of the nanoparticles in the dilute nanofluids was measured with dynamic light scattering and ranged from 110 to 210 nm for Al_2O_3 nanofluids, from 110 to 250 nm for ZrO_2 nanofluids, and from 20 to 40 nm for SiO_2 nanofluids. With these nanofluids we have measured a CHF enhancement of up to 50% in previous experiments.[7] The heaters were flat plates, 5 mm wide, 45 mm long, and 0.05 mm thick and were made of grade 316 stainless steel. We observed that soon after nanofluid boiling is initiated, some nanoparticles precipitate on the heater surface and form irregular porous structures, which do not appear during boiling of pure water (Fig. 1). The energy dispersive spectrometer analysis of the surface confirmed that the porous layer is made of the same material of the nanoparticles used in the experiment. Similar nanoparticle precipitation was observed by other researchers experimenting with nanofluid boiling.[4–6] Various mechanisms of nanoparticle precipitation and adhesion to the heater surface have been hypothesized (e.g., liquid evaporation, surface chemical reactions, electric fields, and dip coating); however, regardless of the mechanism, the presence of a porous layer on the surface can undoubtedly have a significant impact on boiling heat transfer through changes in surface area, surface wettability, and bubble nucleation.

In this letter we intend to answer the following three questions. Does the nanoparticle layer change the wettability of the heated surface? What are the physical mechanisms that cause the wettability change? What are the consequences on nucleate boiling heat transfer and CHF?

In order to investigate surface wettability, the static contact angle θ was measured for sessile droplets of pure water and nanofluids at 22 °C in air on clean surfaces and nanoparticle-fouled surfaces. The sessile droplet method is a well established technique for assessing wetting of a solid by a liquid[8] and has been used routinely in boiling heat transfer studies.[9,10] Low values of the contact angle correspond to high surface wettability. Figure 2 shows that the contact angle decreases from about 70° to about 20° on the fouled surfaces. Such decrease occurs with pure water as well as nanofluid droplets, thus suggesting that wettability is enhanced by the porous layer on the surface, not the nanoparticles in the fluid. In another research, Wasan and Nikolov[11] found that ordering of nanoparticles near the liquid/solid contact line can increase the spreading of nanofluids.

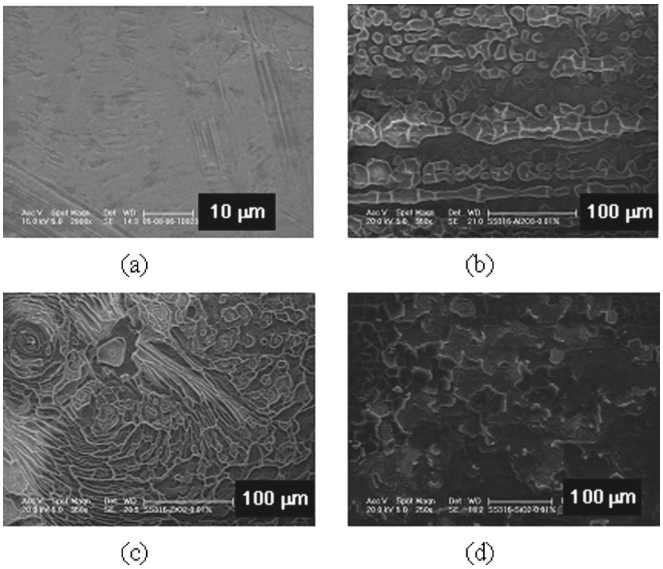

FIG. 1. Scanning electron microscope images of stainless steel surface boiled in (a) pure water, (b) 0.01 vol % Al_2O_3 nanofluid, (c) 0.01 vol % ZrO_2 nanofluid, and (d) 0.01 vol % SiO_2 nanofluid.

[a]Author to whom correspondence should be addressed; electronic mail: jacopo@mit.edu

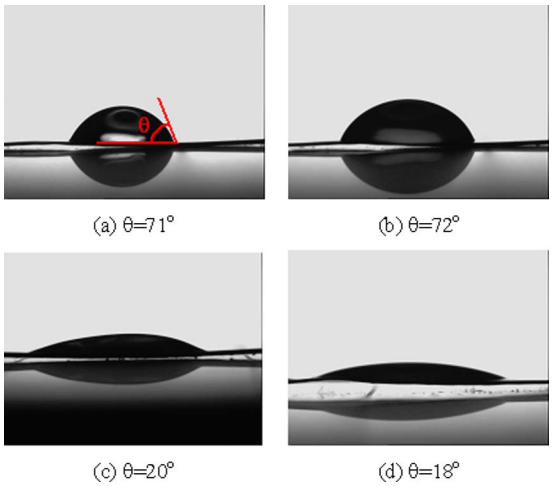

FIG. 2. (Color online) Contact angles of 5 μl sessile droplets on stainless steel surfaces, measured with a Krüss goniometer (uncertainty ±0.1°) equipped with a camera monitor. (a) Pure water droplet on surface boiled in pure water, (b) 0.01 vol % Al_2O_3 nanofluid droplet on surface boiled in pure water, (c) pure water droplet on surface boiled in 0.01 vol % Al_2O_3 nanofluid, and (d) 0.01 vol % Al_2O_3 nanofluid droplet on surface boiled in 0.01 vol % Al_2O_3 nanofluid. Similar results were obtained with the SiO_2 and ZrO_2 nanofluids.

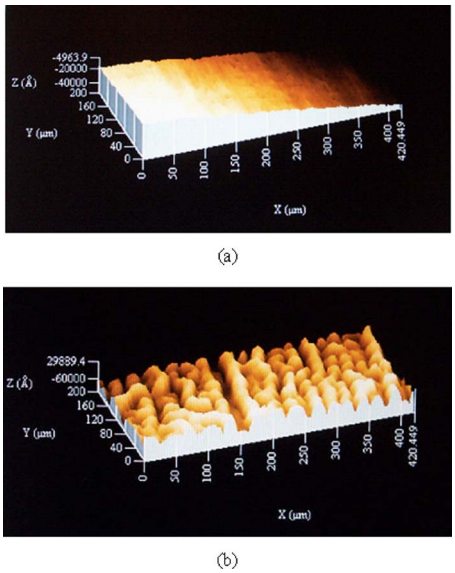

FIG. 3. (Color online) Profilometer images of the stainless steel surface after boiling (a) pure water and (b) 0.1 vol % alumina nanofluid. The rms roughness values are ~0.1 and ~2 μm, respectively. Similar results were obtained with the other nanofluids.

To understand the dramatic enhancement of wettability, we consider Young's equation

$$\cos\theta = \frac{\gamma_{SV} - \gamma_{SL}}{\gamma_{LV}}, \tag{1}$$

which relates the static contact angle to the so-called adhesion tension $\gamma_{SV} - \gamma_{SL}$ and the surface tension γ_{LV}. The adhesion tension of water on clean steel is ~10 mN/m and its surface tension is ~72 mN/m, so Young's equation yields a contact angle of about 82°, which is in reasonable agreement with the measured angle [Fig. 2(a)]. If the surface is not smooth, the effective solid-liquid contact area differs from the smooth contact area. Wenzel[12] defines a roughness factor r as the ratio of the effective contact area to the smooth contact area. The free energy of the solid-liquid interface on a rough surface is then r times the free energy of a perfectly smooth surface with the same apparent contact area. Therefore, Young's equation needs to be modified as follows:

$$\cos\theta^* = \frac{\gamma_{SV} - \gamma_{SL}}{\gamma_{LV}} r = r\cos\theta, \tag{2}$$

where θ^* is the apparent contact angle. Note that the measured contact angles shown in Figs. 2(c) and 2(d) are, in fact, apparent contact angles because of the presence of the porous layer. Equation (2) suggests that the contact angle depends on three parameters, (i) the surface tension (γ_{LV}), (ii) the adhesion tension ($\gamma_{SV} - \gamma_{SL}$) and (iii) the roughness factor. The surface tension of our nanofluids was measured with a Sigma 703 tensiometer and found very close (within ±3%) to that of pure water. On the other hand the adhesion tension of water increases significantly in going from a clean metal to an oxide, e.g., from ~10 mN/m (stainless steel) to ~60 mN/m (alumina). Such change in adhesion tension alone reduces the contact angle to ~34°, as calculated from Eq. (2) assuming $r=1$. This is consistent with other studies showing that surface oxidation decreases the contact angle.[9] The porous layer also increases the effective contact area. Thus the roughness factor r is greater than unity, which also contributes to the contact angle reduction in our case. To evaluate r, we used a Tencor P-10 surface profilometer, which gave the images shown in Fig. 3. The surface boiled in pure water is very smooth, while the surface boiled in nanofluid presents structures consistent with the images of Fig. 1. The estimated surface areas are of the order of 84 000 and 470 000 μm^2 for the surface boiled in pure water and the surface boiled in nanofluid, respectively, resulting in $r \sim 5.6$. This is to be considered an upper bound estimate for r, because it assumes that the pores are completely filled with liquid. In reality the capillary pressure pulls the liquid into the pores until it is balanced by the pressure of the trapped gases. For $r \sim 5.6$ the apparent contact angle decreases to ~39°, as calculated from Eq. (2) with nominal adhesion tension (~10 mN/m) and surface tension (~72 mN/m). In summary, a simple analysis of the modified Young's equation suggests that the enhancement in wettability (decrease in contact angle) is caused by a combination of two effects, i.e., an increase of adhesion tension and an increase of surface roughness. Both effects are at work and both effects are large enough to cause the observed reduction in contact angle.

We shall now discuss the impact of wettability enhancement on boiling heat transfer in nanofluids. Activation of microcavities on the surface is generally described by the criterion of $\theta \geqslant \beta$, where β is the opening angle of an idealized conical cavity. According to Yang and Kim,[13] the number of active cavities per unit surface area, N_a, is

$$N_a = N_s \int_{R_{min}}^{R_{max}} \varphi(R) dR \int_0^{\theta} \phi(\beta) d\beta, \tag{3}$$

where N_s is the cavity areal density, R_{max} and R_{min} are the maximum and minimum active cavity radii, respectively, $\varphi(R)$ is the cavity radius distribution function, and $\phi(\beta)$ is the distribution function for the cavity opening angle. Therefore, a decrease of the contact angle, as was observed on nanoparticle-fouled surfaces, will tend to decrease the number of active cavities. Plausibly this contributes to the decrease in bubble nucleation in nanofluids with respect to pure

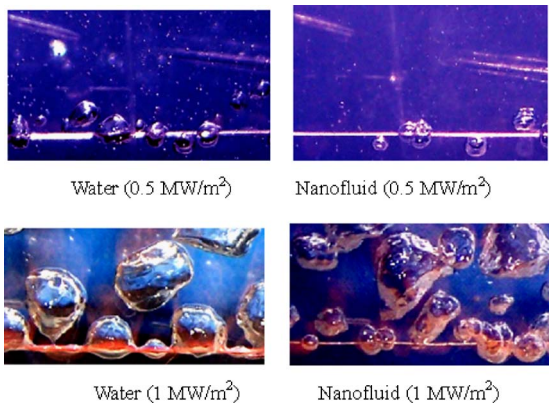

FIG. 4. (Color online) Nucleate boiling of pure water (left) and 0.01 vol % alumina nanofluid (right) at the same heat flux on an electrically heated 0.25 mm diameter stainless steel wire. Note the fewer bubble nucleation events (at 0.5 MW/m^2) and delayed CHF (at 1.0 MW/m^2) in the nanofluid.

water, as shown in Fig. 4 and also observed in other studies.[4,7,14]

Surface wettability also profoundly affects CHF. While a generally valid theory of CHF does not exist, the most credible hypotheses postulate that dry patches (or hot spots) develop on the heated surface at high values of the heat flux.[15–17] These dry patches can be rewetted or can irreversibly overheat, which causes CHF. Clearly, an increase in surface wettability promotes dry patch rewetting, thus delaying CHF. To estimate the impact of the observed contact angle change on CHF, we can use the simple model of Sadasivan *et al.*[18] This model postulates that bubbles growing at neighboring active cavities can coalesce laterally at a certain stage during the growth phase before they depart from the surface. A certain volume of liquid is trapped between the vapor bubbles below the plane of coalescence [Fig. 5(a)]. Above the plane of coalescence, the vapor may form a large mushroom-shaped bubble that hovers over the surface for a

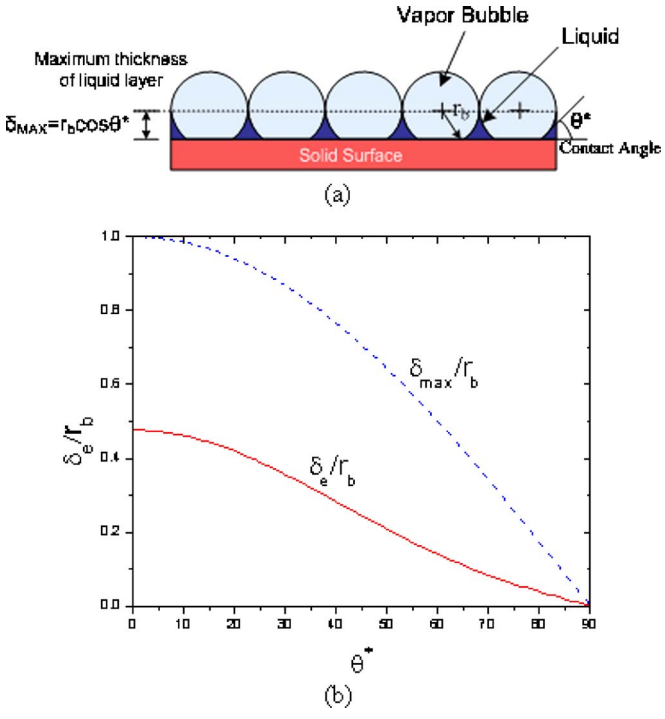

FIG. 5. (Color online) CHF phenomena. (a) Liquid layer concept of Sadasivan *et al.* (Ref. 18). (b) Liquid layer thickness vs contact angle.

time τ_h. The bubbles are assumed to have uniform size with radius r_b, and be uniformly distributed over the heater surface. Therefore, for a $2r_b \times 2r_b$ unit cell the volume of liquid trapped below the plane of coalescence is $4r_b^3 \cos\theta^* - \left[\frac{1}{3}\pi r_b^3(3\cos\theta^* - \cos^3\theta^*)\right]$. The equivalent thickness of the liquid film is then calculated assuming uniform spreading of the trapped liquid over the surface as

$$\delta_e = r_b\left[\cos\theta^* - \frac{\pi}{12}(3\cos\theta^* - \cos^3\theta^*)\right]. \quad (4)$$

For given r_b, the liquid film thickness increases with decreasing contact angle [Fig. 5(b)]. The time to dry out the liquid film, τ_d, can be estimated from the energy balance at the surface as $\tau_d = \delta_e \rho_f h_{fg}/q''$ where q'', ρ_f and h_{fg} are the heat flux, liquid density, and evaporation heat, respectively. Sadasivan *et al.* hypothesize that CHF occurs if $\tau_d < \tau_h$. Since τ_h depends mostly on hydrodynamics and only weakly on the heat flux,[19] the increase in τ_d has a direct effect on CHF, i.e., the value of the heat flux at which CHF occurs is proportional to τ_d. Equation (4) suggests that a contact angle reduction from 70° to 20° would increase the liquid layer thickness about fourfold, which results in a fourfold increase of the dryout time and thus in roughly a fourfold increase of the CHF. Recognizing that the CHF enhancement reported in the literature is of the same order of magnitude (up to 200%) but not quite so large, we can, however, conclude that the liquid layer model points to a strong nexus between CHF enhancement and surface wettability improvement caused by nanoparticle deposition.

The following sponsors are gratefully acknowledged: AREVA (PO CP04-0217), the Idaho National Laboratory (Contract No. 063, Release 18), the Nuclear Regulatory Commission (NRC-04-02-079), the DOE Innovation in Nuclear Infrastructure and Education Program (DOE-FG07-02ID14420), the Korea Science and Engineering Foundation for one of the author's (S.J.K.) doctoral fellowship and the Korea Research Foundation (KRF-2005-214-D00400) for another author's (I.C.B.) postdoctoral fellowship.

[1] J. A. Eastman, S. U. Choi, S. Li, W. Yu, and L. J. Thompson, Appl. Phys. Lett. **78**, 718 (2001).
[2] S. M. You, J. H. Kim, and K. H. Kim, Appl. Phys. Lett. **83**, 3374 (2003).
[3] P. Vassallo, R. Kumar, and S. D'Amico, Int. J. Heat Mass Transfer **47**, 407 (2004).
[4] I. C. Bang and S. H. Chang, Int. J. Heat Mass Transfer **48**, 2407 (2005).
[5] D. Milanova and R. Kumar, Appl. Phys. Lett. **87**, 233107 (2005).
[6] H. Kim, J. Kim, and M. Kim, Nuclear Engineering and Technology **38**, 61 (2006).
[7] S. J. Kim, B. Truong, J. Buongiorno, L. W. Hu, I. C. Bang, Proceedings of ICAPP '06, Reno, NV, 4–8 June 2006, (http://www.ans.org/store/vc-prcd).
[8] P. G. de Gennes, Rev. Mod. Phys. **57**, 827 (1985).
[9] C. H. Wang and V. K. Dhir, J. Heat Transfer **115**, 659 (1993).
[10] Y. Takata, S. Hidaka, M. Masuda, and T. Ito, Int. J. Energy Res. **27**, 111 (2003).
[11] D. T. Wasan and A. D. Nikolov, Nature (London) **423**, 156 (2003).
[12] R. N. Wenzel, J. Phys. Colloid Chem. **53**, 1466 (1949).
[13] S. R. Yang and R. H. Kim, Int. J. Heat Mass Transfer **31**, 1127 (1988).
[14] S. Das, N. Putra, and W. Roetzel, Int. J. Heat Mass Transfer **46**, 851 (2003).
[15] Y. Haramura and Y. Katto, Int. J. Heat Mass Transfer **26**, 389 (1983).
[16] J. M. Ramilson and J. H. Lienhard, J. Heat Transfer **109**, 746 (1987).
[17] T. G. Theofanus, T. N. Dinh, J. P. Tu, and A. T. Dinh, Exp. Therm. Fluid Sci. **26**, 793 (2002).
[18] P. Sadasivan, P. R. Chappidi, C. Unal, and R. A. Nelson, *Pool and External Flow Boiling* (ASME, New York, 1992), p. 135.
[19] Y. Katto and S. Yokoya, Int. J. Heat Mass Transfer **11**, 993 (1968).